

## Polystyrene nanodroplets

This article has been downloaded from IOPscience. Please scroll down to see the full text article.

2001 J. Phys.: Condens. Matter 13 4915

(<http://iopscience.iop.org/0953-8984/13/21/318>)

View [the table of contents for this issue](#), or go to the [journal homepage](#) for more

Download details:

IP Address: 171.66.16.226

The article was downloaded on 16/05/2010 at 13:22

Please note that [terms and conditions apply](#).

# Polystyrene nanodroplets\*

Ralf Seemann<sup>1</sup>, Karin Jacobs<sup>1</sup> and Ralf Blossey<sup>2</sup>

<sup>1</sup> Universität Ulm, Abteilung Angewandte Physik, Albert-Einstein-Allee 11, D-89069 Ulm, Germany

<sup>2</sup> Universität Essen, Fachbereich Physik, D-45117 Essen, Germany

Received 1 December 2000, in final form 14 February 2001

## Abstract

We study, in both theory and experiment, the shape of sessile, nanometre-sized droplets generated from the rupture of unstable or metastable films of a polymer melt (polystyrene) on Si wafers. We find perfect agreement of the droplet shapes determined by atomic force microscopy with simple exact scaling results obtained from an effective interface displacement model for droplets in the ‘macroscopic’ limit. The experimentally determined line tension is of the magnitude expected from the interface model approach. Our results thus corroborate other recent findings on the qualitative and quantitative validity of the interface model approach to wetting phenomena.

## 1. Introduction

The properties of liquids at solid surfaces are a topic of current interest from both the fundamental and the applied points of view. Much progress has recently been achieved due to new methods of controlled surface preparation and a close interaction between experiment and theory [1, 2]. The simplest physical system in this context certainly is that of sessile liquid droplets placed on solid substrates—droplets at surfaces are indeed a ubiquitous sight in everyday life! However, despite the apparent simplicity of these systems a rigorous mathematical treatment of their properties is far from being trivial, as can e.g. be inferred from Robert Finn’s book on *Equilibrium Capillary Surfaces* [3].

The equilibrium shape of a sessile droplet at a wall is determined by the tendency of the liquid to minimize its surface area (or, equivalently, its surface free energy). In the simplest configuration a sessile liquid droplet on a smooth horizontal plane will therefore be a spherical cap, i.e., a full sphere out of which a section has been cut by the solid substrate. This liquid ‘cap’ meets the solid at the so-called contact angle  $\theta$  determined by Young’s relation

$$\cos \theta = \frac{\gamma_{sv} - \gamma_{sl}}{\gamma_v} = 1 + \frac{S}{\gamma_v} \quad (1)$$

in which the symbols  $\gamma_{..}$  denote the interfacial tensions between the solid, vapour and liquid phases.  $S$  is the spreading coefficient, defined as  $S \equiv \gamma_{sv} - (\gamma_{sl} + \gamma_{lv})$ . For a sessile droplet,  $0 < \theta < 180^\circ$ , so  $S < 0$ . This situation is called ‘partial wetting’.

\* We dedicate this paper to Richard Bausch on the occasion of his 66th birthday.

In more general situations, additional forces compete with the interfacial tensions which are the main agents in determining the shape of a sessile drop. These forces are gravity and long-ranged intermolecular forces not accounted for by the interfacial tensions, like van der Waals forces [4]. Gravity is most relevant for large droplets in which it flattens the drop around its central height  $F$ . A simple estimate of the relevance of gravity for the droplet shape is provided by the capillary length  $a \equiv \sqrt{\gamma_{lv}/g_0\rho}$  where  $g_0$  is the gravitational acceleration and  $\rho$  the liquid density. Typically,  $a$  is a length at least of the order of microns such that for  $F \leq a$  gravity will be negligible.

Here we focus on the effect of intermolecular forces on the shape of sessile droplets. Intermolecular forces are more interesting than gravity from the point of view of wetting phase transitions which are commonly controlled by these forces. A simple question can then be posed: do intermolecular interactions, which typically become appreciable in liquid films of about 100 nm thickness and less, matter for the shape of a drop of this size like gravitational forces do for droplets thicker than microns?

In this paper, we address this question first theoretically. For this we employ an effective interface model which has recently proven highly successful in both qualitative and quantitative descriptions of wetting and dewetting phenomena (see the discussion section). We carefully review a number of physical and mathematical aspects associated with a liquid partially wetting a solid surface and, subsequently, we report on the validation of the theoretical results in experiments on nanometre-sized polymer droplets whose shape we have determined by atomic force microscopy (AFM).

## 2. Theory

### 2.1. The effective interface Hamiltonian

In order to determine the shape of a sessile droplet sitting at a solid surface we employ the effective interface model approach based on the Hamiltonian [5–7]

$$\mathcal{H}[f] = \int d^2x [\gamma_{lv}\sqrt{g} + V(f) - \lambda f]. \quad (2)$$

In the model defined by equation (2), the field variable  $f(x)$  denotes the local height of the liquid–vapour interface above the solid. The first term in equation (2) is the capillary energy of the liquid–vapour interface in a Monge representation with  $g = 1 + (\nabla f)^2$ . The second term in  $\mathcal{H}[f]$  is the surface free-energy density of a flat film, more commonly called the effective interface potential  $V(f)$ . Finally, the last term in equation (2) either corresponds to a chemical potential difference between bulk liquid and vapour phases,  $\lambda \equiv \Delta\mu$ , or to a Lagrange parameter associated with a fixed droplet volume  $\Omega \equiv \int d^2x f(x)$ . We now turn to a more detailed discussion of these different contributions.

*2.1.1. The capillary contribution.* Within the interface model approach, the capillary contribution to equation (2) is most often approximated by a squared-gradient term  $(\gamma_{lv}/2)(\nabla f)^2$ . This term is usually sufficient whenever only spatial variations of the liquid–vapour interface on long length scales are of interest, for which the gradients of  $f$  are generally small. For spatial variations of the interface on small scales, this approximation will of course be insufficient.  $\mathcal{H}[f]$  then needs to be replaced by a non-local functional which is obtained as an effective description starting from a more microscopic density functional theory [8, 9]. We will adopt the squared-gradient approximation in our theoretical calculations (but we will see in comparison with the experimental results when this approximation will not work any longer).

**2.1.2. The effective interface potential.** The effective interface potential is the surface free-energy density of a homogeneous (flat) film at which in general both short- and long-range forces act. In the case of a system with a first-order wetting transition,  $V(f)$  has two minima which correspond to either a flat microscopic (i.e., a finite) or a macroscopic (i.e., an infinitely thick) wetting film. In the case addressed here, a thick film is metastable with respect to the thin film, since the thin-film minimum is the globally stable one. Alternatively, a thick film can be completely unstable on the substrate. This is the case when  $V(f)$  displays only a thin-film minimum.

These two situations are shown in figure 1. For both types of system,  $V(f)$  decays for large thicknesses algebraically to zero, either from above or below. This decay is determined by the van der Waals interactions in the system, which in the case of negligible retardation effects act as  $V(f) \sim f^{-2}$ . The notion ‘effective’ in the terminology of the interface model refers to the fact that this potential contains entropic contributions and hence its coefficients are in general temperature dependent. The Hamaker ‘constant’, which is the amplitude of the long-ranged decay of the van der Waals contribution to  $V(f)$ , e.g., may in fact even change its sign upon a temperature change and thus completely alter the character of the long-range forces [10].

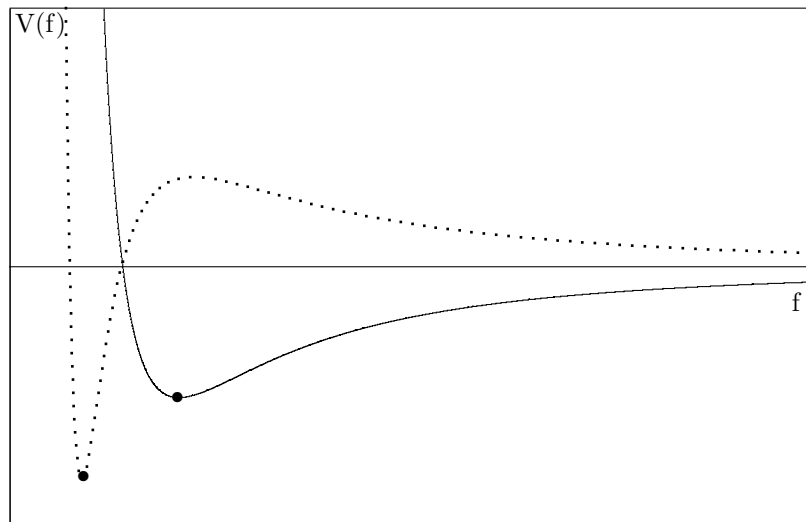


**Figure 1.** The effective interface potential  $V(f)$  with metastable and unstable thick-film states. The thin-film minimum at  $f = f_0$  is indicated by ●.

**2.1.3. The chemical potential/the Lagrange parameter.** The last term in equation (2) contains the chemical potential difference  $\Delta\mu$  between a bulk liquid and a bulk vapour phase in the vicinity of a solid wall. Supposing that the system is in its thin-film state (e.g. in the case of a wettable surface at temperatures below the wetting temperature), we have to differentiate between physically different situations which are, however, mathematically rather similar.

- (1) If  $\Delta\mu \leq 0$ , the gas phase is stable in bulk and a thin (microscopic) wetting layer covers the substrate. A droplet can nevertheless sit on the substrate if its volume is prescribed in the surface free energy by the introduction of a Lagrange parameter.

Physically this volume constraint can be violated, e.g. if the liquid is volatile [11]. In this case, the liquid will leave the substrate by evaporation. As an alternative possibility the liquid can ‘flow’ into the thin-film state via spreading of the droplet if allowed by the viscosity of the liquid. The droplet therefore is in principle metastable with respect to the thin film [12].

- (2) If  $\Delta\mu > 0$ , the bulk liquid phase is stable in bulk. A sessile droplet can then appear as a metastable configuration at the wall and is either a subcritical, supercritical, or critical droplet with respect to the formation of the stable liquid phase near the wall.

We will neglect gravitational contributions to the effective interface model in the following discussion of sessile droplets. If included, they lead to a term  $\int d^2x \rho g_0 f^2/2$  in the interface Hamiltonian of equation (2). The wetting phase diagram with the inclusion of this term has recently been determined [13]. The main effect of the presence of gravity is to remove the wetting transition completely, leaving only prewetting transitions.

We finally note that the description of the approach to the wetting transition at coexistence from temperatures below the transition can be treated equivalently within the interface displacement description and the classic droplet picture, involving the vanishing of the contact angle  $\theta$ . Both can be formulated within the interface model. The main difference between the two descriptions is that in the former, the system is considered in a grand-canonical description, leaving the number of particles in the thin film unfixed. By contrast, a droplet is to be considered in the canonical ensemble, its volume (hence its particle number) being held constant.

## 2.2. Sessile droplets from an interface displacement model

The shape of a sessile droplet at a solid wall is obtained from equation (2) via the functional variation  $\delta\mathcal{H}/\delta f(r) = 0$ , where the assumption of cylindrical symmetry of the droplet is expressed in the radial dependence of the droplet height  $f$ . The resulting variational equation reads

$$\gamma_{lv} \left( f''(r) + \frac{1}{r} f'(r) \right) = V'(f) - \lambda. \quad (3)$$

Suitable boundary conditions for a sessile drop are  $f'(0) = 0$  and  $f(\infty) = f_0$ .

In order to generate a sessile droplet, one needs  $\lambda > 0$  such that for large values of  $f$  the liquid phase is favoured. The full potential  $V(f) - \lambda f$  decays linearly in  $f$  to negative infinity (i.e., is unbounded below). In this case there is a droplet solution to equation (3) which fulfils the desired boundary conditions. This is easily seen by consideration of the mechanical analogy to equation (3). If  $f$  is interpreted as the trajectory of a classical particle running in the inverted potential  $\lambda f - V(f)$  in ‘time’  $r$ , the desired solution is obtained when the initial condition  $f(r=0) \equiv F$  is found which ‘shoots’ the particle with zero initial velocity to the local maximum of the inverted potential at  $f = f_0$ . For  $f(0) < F$  and  $f(0) > F$ , the particle will either undershoot or overshoot [11, 14].

Due to the non-linear nature of the interface potential, a closed analytic expression for the droplet profile cannot be obtained. The situation, however, simplifies in the limit  $\lambda \rightarrow 0$ . In this limit the initial condition  $F$  will be pushed further and further out to infinity, so the particle will spend the largest portion of its course in the linear region of the potential. One might therefore be tempted to neglect  $V(f)$  altogether as an approximation, since it remains relevant only near the foot of the droplet. In doing so we also have to modify the second boundary condition by means of the extrapolation  $f(R) = 0$ , introducing the droplet radius at the wall,  $R$ . The solution of the full equation (3) converges to the analytic approximation in the limit

$\lambda \rightarrow 0$  [14]. With this approximation, equation (3) becomes linear and is easily solved by a ‘macroscopic’ profile [14]

$$f(r) = F(1 - (r/R)^2) \quad (4)$$

where

$$F = 2|S|\lambda^{-1} \quad R = 2\sqrt{2\gamma_v|S|\lambda^{-1}} \quad (5)$$

are the droplet height and the droplet radius, respectively. Note that in the parabolic approximation, the relation between contact angle and spreading coefficient is given by

$$S = \gamma_v\theta^2/2 \quad (6)$$

which follows from the expansion of the  $\cos\theta$  in equation (1). The ratio of  $F$  and  $R$  thus is independent of  $\lambda$ :

$$\frac{F}{R} = \sqrt{\frac{|S|}{2\gamma_v}} \quad (7)$$

and hence is, via equation (6), a function of contact angle  $\theta$ .

In addition we obtain the excess free energy of the sessile droplet,

$$\mathcal{E} \equiv \mathcal{H}[f(r)] - \mathcal{H}[f = 0].$$

It is given by the expression [14]

$$\mathcal{E} = 8\pi\gamma_v\left(\frac{|S|}{\lambda}\right)^2 = \pi|S|R^2. \quad (8)$$

### 3. Experiment

We have studied the profiles of nanometre-sized sessile droplets of atactic polystyrene (PS, purchased from Polymer Laboratories, Church Stratton, UK) with a molecular weight of  $2.05 \text{ kg mol}^{-1}$  and a polydispersity of  $M_w/M_n = 1.05$ . A toluene solution of polystyrene is spin coated on Si wafers, resulting in uniform polystyrene films. Depending on the polymer concentration of the solution and the rotational speed, 4–15 nm thick films were prepared. Subsequently, the samples were heated to temperatures above the glass transition. In the case of a negative spreading coefficient,  $S < 0$ , the film is not stable and dewets the surface [15–17], leaving behind a set of sessile droplets (see figure 2).

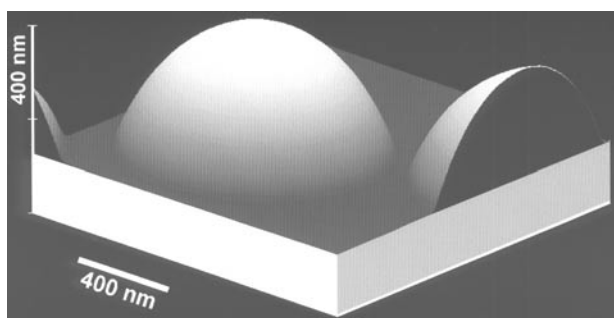


**Figure 2.** Sessile PS ( $2.05 \text{ kg mol}^{-1}$ ) droplets on an OTS wafer.

The Si wafers were prepared in two ways, resulting in different wetting properties. The first series of Si wafers, purchased from Silchem Handelsgesellschaft mbH Freiberg, Germany,

have an extremely thick silicon oxide layer of 191(1) nm on the surface, as determined by ellipsometry. From now on, we call these samples ‘SiO wafers’. After the SiO wafer was cut, the samples were cleaned with a ‘snow jet’ (a fast CO<sub>2</sub> jet consisting in part of CO<sub>2</sub> crystals; Tectra GmbH, Frankfurt/Main, Germany) to remove microscopic contaminations. Chemical residues were removed in a subsonic cleaner by immersing the samples into ethanol, acetone and toluene. Additionally, the SiO samples were treated with ‘piranha solution’, i.e., a 1:1 mixture of concentrated sulphuric acid and hydrogen peroxide (35%). Finally, the samples were washed in hot *Millipore*<sup>TM</sup> water and spin coated with a toluene solution of PS. The SiO wafers prepared in this way are non-wettable for PS films [18].

The second series of Si wafers, purchased from Wacker GmbH, Burghausen, Germany, were hydrophobized by a monolayer of OTS (octadecyl-trichlorosilane) [19, 20]. After the wafers were cut into 1 cm<sup>2</sup> pieces they were cleaned in a subsonic cleaner with organic solvents as described above. In the following, we call that substrate the ‘OTS wafer’. On an OTS wafer, the PS film cannot be prepared by spin coating directly onto the substrate due to the large contact angle of toluene on OTS. Here, the PS solution is spun onto freshly cleaved mica sheets. From there the films were floated onto a surface of clean, *Millipore*<sup>TM</sup> water and picked up with the OTS wafers.

The sessile droplets, obtained after dewetting of the polystyrene film, were characterized by AFM in *Tapping Mode*<sup>TM</sup>. Contact angles were determined on the basis of radial cross sections of the droplets. Here, two methods were applied: (i) determination of the slope at the three-phase contact line and (ii) determination from a fit of a spherical cap to the data (figure 3). For the first method, a large number of AFM data points are necessary; otherwise the insufficient spatial resolution will always lower the values of the contact angle. The two different methods yield, within their respective error bars of maximally 1°, identical values.

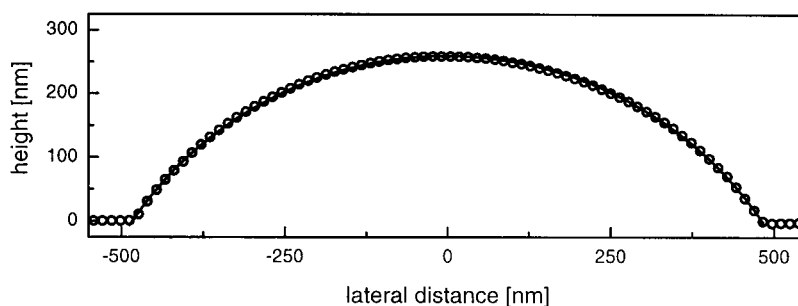


**Figure 3.** An AFM scan of a sessile droplet profile and its fit to a parabola.

In figure 4 we have plotted the ratio of the scaling parameter central height of the droplet  $F$  and the droplet radius  $R$  at the surface, equation (7), as a function of contact angle. We obtain two clusters of data. Droplets on the SiO wafers have a contact angle of 6.9(5)° with a height of about 20–40 nm. Droplets on the OTS wafer have a contact angle of about 58(1)° and a central height of about 200–550 nm. Solid lines correspond to the scaling result for a parabolic droplet profile as given by equation (7), and the correction seen for a spherical cap profile.

#### 4. Discussion

Figure 4 (together with the results in equation (7)) is the main result of this paper. The experimental data clearly demonstrate that the profile of a nanosized sessile droplet is not

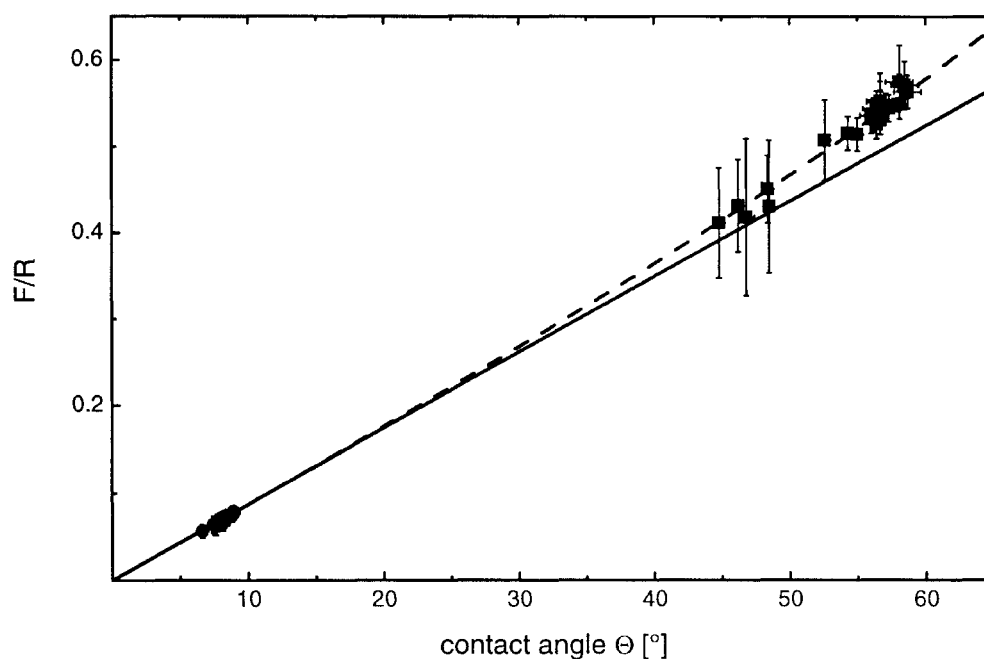


**Figure 4.** The scaling of the droplet shape:  $F/R$  as a function of contact angle.

sensitive to the intermolecular interactions, so the approximations used in obtaining the scaling results, equations (5), are justified. Although the droplets have heights well within the range where intermolecular forces act, there is no need to invoke more microscopic details than are contained in the interface model description to characterize them. For the droplets with small contact angles, we find that the result obtained from the squared-gradient expression for the surface free energy characterizes their shapes well. The shapes of the drops with larger contact angles are spherical caps, so the full Monge expression for the surface free energy has to be retained. Consistent with our approximations, we see no deviations of the shapes that might resemble the flattening effect of gravitational forces on macroscopic droplets, although dispersion forces of the order of 30 N act on them.

However, in line with our expectations, deviations from the almost macroscopic droplet shape due to intermolecular forces do occur in the vicinity of the three-phase contact line with line tension  $\tau$  for droplet profiles in which the contact line has a large curvature  $\kappa$  [21]. Here, the contact angle obeys the modified Young equation [22, 23]

$$\cos \theta_{\tau} = \cos \theta - \frac{\tau \kappa}{\gamma_{lv}} \quad (9)$$

which can be derived from the effective interface model [22], also giving an explicit expression for  $\tau$  [22, 25]. To check for this correction for our droplets, we took the AFM data on the PS droplets on the SiO wafers shown in figure 3 and determined the line tension according to equation (9). Figure 5 shows the resulting  $\cos \theta / \kappa$  diagram. With a value for the surface tension  $\gamma_{lv} = 30.8 \text{ mN m}^{-1}$  we obtain a value for  $\tau$  of the order of  $-10^{-11} \text{ J m}^{-1}$ . Thus, the magnitude of  $\tau$  that we find agrees well with those predicted theoretically from the interface model approach [21], while it significantly deviates from those obtained with optical methods, which is of the order of  $-10^{-6} \text{ J m}^{-1}$  [24, 26].



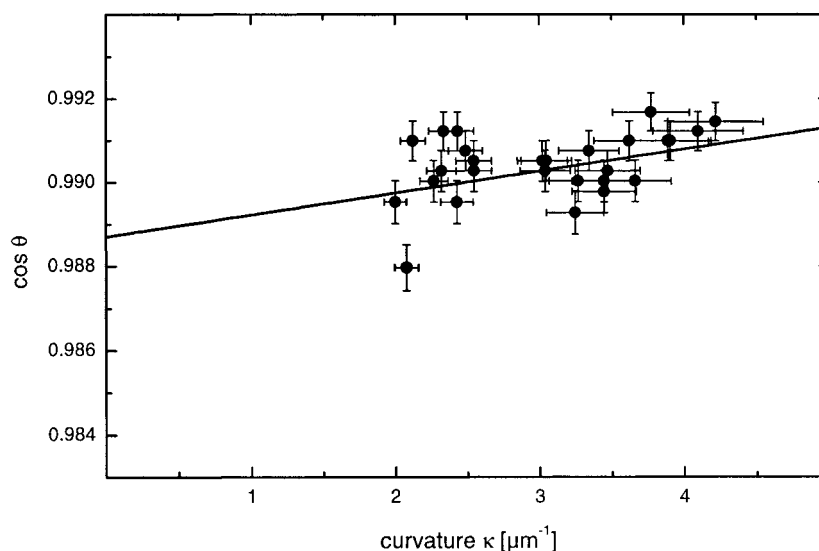


**Figure 5.** The line tension of a polystyrene droplet on a Si wafer.

Finally, we mention that significant effects of intermolecular interactions also show up for critical droplets in overheated wetting layers in which the divergence of the line tension  $\tau$  near the wetting transition significantly contributes to the lifetime of the overheated thin wetting layer [27].

To conclude, our finding corroborates other recent results on the quantitative validity of the effective interface potential approach. The effective interface model has been able to qualitatively and quantitatively explain first-order and critical wetting transitions [10], dewetting transitions of polymer films [17], measurements of the contact line tension [21], nucleation of wetting layers and their subsequent growth [27]. We are confident that more results are soon to follow.

### Acknowledgments

This work was supported by the German Research Society DFG under the Schwerpunktprogramm ‘Benetzung und Strukturbildung an Grenzflächen’ (grants Ja905/1-2 and B1356/2-1). Ralf Blossey gratefully acknowledges support from the DFG under the Leibniz programme (grant Di387/2). Moreover, we acknowledge generous support by Wacker Chemitronics, Burghausen, Germany, in providing the Si wafers.

### References

- [1] Herminghaus S, Fery A, Schlagowski S, Jacobs K, Seemann R, Gau H, Mönch W and Pompe T 2000 *J. Phys.: Condens. Matter* **11** A57
- [2] Herminghaus S *et al* 1998 *Science* **28** 916
- [3] Finn R 1986 *Equilibrium Capillary Surfaces* (New York: Springer)
- [4] Israelachvili J 1992 *Intermolecular and Surface Forces* (New York: Academic)
- [5] De Gennes P G 1985 *Rev. Mod. Phys.* **57** 827
- [6] Schick M 1990 *Liquids at Interfaces (Les Houches Session XLVII, 1988)* ed J Charvolin, J F Joanny and J Zinn-Justin (Amsterdam: North-Holland)

- [7] Dietrich S 1990 *Phase Transitions and Critical Phenomena* vol 12, ed C Domb and J L Lebowitz (London: Academic)
- [8] Mecke K R and Dietrich S 1999 *Phys. Rev. E* **59** 6766
- [9] Fradin C, Braslau A, Luzet D, Smilgies D, Alba M, Boudet N, Mecke K R and Daillant J 2000 *Nature* **403** 871
- [10] Shahidzadeh N, Bonn D, Ragil K, Broseta D and Meunier J 1998 *Phys. Rev. Lett.* **80** 3992
- [11] Blossey R 1995 *Int. J. Mod. Phys. B* **9** 3489
- [12] Ball P 1989 *Nature* **338** 624
- [13] Blossey R and Oligschleger C 1999 *J. Colloid Interface Sci.* **209** 442
- [14] Bausch R and Blossey R 1993 *Phys. Rev. E* **48** 1131
- [15] Vrij A 1966 *Discuss. Faraday Soc.* **42** 23
- [16] Reiter G 1992 *Phys. Rev. Lett.* **68** 75
- [17] Jacobs K, Herminghaus S and Mecke K R 1998 *Langmuir* **14** 965
- [18] Seemann R, Herminghaus S and Jacobs K 2001 *J. Phys.: Condens. Matter* **13**
- [19] Wasserman S R, Tao Y and Whitesides G M 1989 *Langmuir* **5** 1075
- [20] Brzoska J B, Ben Azouz I and Rondelez F 1994 *Langmuir* **10** 4367
- [21] Pompe T and Herminghaus S 2000 *Phys. Rev. Lett.* **85** 1930
- [22] Dobbs H 1999 *Int. J. Mod. Phys. B* **13** 3255
- [23] For a generalization of the modified Young equation to droplets on heterogeneous substrates under gravity, see Swain P S and Lipowsky R 1998 *Langmuir* **14** 6772
- [24] Amirfazli A, Kwok D Y, Gaydos J and Neumann A W 1998 *J. Colloid Interface Sci.* **205** 1
- [25] Indekeu J O 1994 *Int. J. Mod. Phys. B* **8** 309
- [26] de Gennes P G 2000 Two remarks on wetting and emulsions *Preprint cond-mat/0009259*
- [27] Bonn D, Bertrand E, Meunier J and Blossey R 2000 *Phys. Rev. Lett.* **84** 4661